

Electron-impact excitation of molecular nitrogen. II. Vibrationally resolved excitation of the $C^3\Pi_u(v')$ state

C. P. Malone,^{1,2} P. V. Johnson,¹ I. Kanik,¹ B. Ajdari,² S. S. Rahman,³ S. S. Bata,⁴ A. Emigh,⁵ and M. A. Khakoo²

¹*Jet Propulsion Laboratory, California Institute of Technology, 4800 Oak Grove Drive, Pasadena, California 91109, USA*

²*Department of Physics, California State University, Fullerton, California 92834, USA*

³*Department of Ecology and Evolutionary Biology, University of California–Los Angeles, Los Angeles, California 90024, USA*

⁴*Brea-Olinda High School, 789 Wildcat Way, Brea, California 92821, USA*

⁵*Fullerton Union High School, 201 East Chapman Avenue, Fullerton, California 92832, USA*

(Received 19 November 2008; published 11 March 2009)

Vibrationally resolved differential cross sections (DCSs) for electron impact from the $X^1\Sigma_g^+(v''=0)$ ground-state level in N_2 are presented for excitation of the $C^3\Pi_u(v')$ state, where $v'=0, 1, 2, 3$, and 4. DCSs for the full $C^3\Pi_u(v')$ state, where $v'=0-4$, are also presented. The vibrationally resolved DCSs were obtained from energy-loss spectra in the region of 10.75 to 12.75 eV measured at incident energies of 13, 15, 17.5, 20, 25, 30, 50, and 100 eV and for scattering angles ranging from 5° to 130° . Relative excitation probabilities for the vibrational levels of the $C^3\Pi_u$ state are shown to demonstrate non-Franck-Condon behavior for excitation energies less than approximately 50 eV. These results are compared with existing measurements.

DOI: 10.1103/PhysRevA.79.032705

PACS number(s): 34.80.Gs, 34.50.Bw, 33.20.Tp, 79.20.Uv

I. INTRODUCTION

Electron impact on molecular nitrogen has received a significant amount of recent attention (e.g., see Refs. [1–4]) largely due to photon emissions in nitrogen dominated atmospheres of the Earth and satellites of planets such as Titan and Triton and its importance in gaseous discharges. Recent calculations [5–7] for e^-+N_2 cross sections have been obtained for excitation of the $A^3\Sigma_u^+$, $B^3\Pi_g$, $W^3\Delta_u$, $B'^3\Sigma_u^-$, $a'^1\Sigma_u^-$, $a^1\Pi_g$, $w^1\Delta_u$, and $C^3\Pi_u$ electronic states from the $X^1\Sigma_g^+(v''=0)$ ground state. The most recent experimental electron energy loss derived data for these excitation processes was from our group [8–12], which also includes the excitation of the $a''^1\Sigma_g^+$, $b^1\Pi_u$, $c_3^1\Pi_u$, $o_3^1\Pi_u$, $b'^1\Sigma_u^+$, $c_4^1\Sigma_u^+$, $G^3\Pi_u$, and $F^3\Pi_u$ states from the $X^1\Sigma_g^+(v''=0)$ ground state.

Excitation of the $C^3\Pi_u$ state of N_2 gives rise to the intense emissions of the $C^3\Pi_u \rightarrow B^3\Pi_g$ second negative band system [13], making it an important process in atmospheric energy transfer. The majority of previous efforts (e.g., Refs. [9,14–16]) at unfolding the complex electron energy-loss spectra of N_2 , including efforts to determine $C^3\Pi_u$ state differential cross sections (DCSs), have relied on Franck-Condon factors (FCFs) to simplify the analysis. However, the $C^3\Pi_u$ valence state is electrostatically coupled to the $C'^3\Pi_u$ valence-state continuum [17], casting doubt on the validity of the Franck-Condon principle as applied to the excitation of the $C^3\Pi_u(v')$ state vibrational levels. For this reason, we have revisited the $C^3\Pi_u$ state. Similar to Zubek and King [18] and Khakoo *et al.* [10], who did not rely on FCFs in their electron energy-loss unfolding, we have obtained DCSs for the excitation of the $C^3\Pi_u$ state in N_2 from the $X^1\Sigma_g^+(v''=0)$ ground-state level. Here, the $C^3\Pi_u$ state was studied with the vibrational levels treated independently in the energy-loss-spectrum unfolding. This paper focuses on the effects of nuclear motion on the differential excitation cross sections for the $C^3\Pi_u$ state vibronic levels and their relative excitation probabilities (REPs) instead of the DCSs

for excitation of the $C^3\Pi_u$ (“full” state, $v'=0-4$) electronic state, which can be found in Paper I (Malone *et al.* [19]) of this series.

II. EXPERIMENT

Details of our experimental setup and procedure are described in Paper I (Ref. [19]) of this publication series and discussed further in Khakoo *et al.* [9,10]. Of note, the $C^3\Pi_u$ state was unfolded from the energy-loss spectra with its vibrational levels treated as independent features (see Table I of Malone *et al.* [19]). Normalization of our DCSs was undertaken in the same manner as in Paper I from the $C^3\Pi_u$ (full, $v'=0-4$) state DCSs using the determined REPs for the $C^3\Pi_u$ state.

III. RESULTS AND DISCUSSION

Our DCSs and associated experimental uncertainty estimations are listed in Table I. These DCSs are compared with existing measurements in Fig. 1. Tables II and III give the REPs of the vibrational levels. Here, Table II presents the REP data as a percentage of the total (full, $v'=0-4$) $C^3\Pi_u$ state excitation and Table III presents renormalized REP data, such that the REP for the $v'=0$ level is unity. The REPs listed in Tables II and III only involve a subset of the uncertainties discussed in Paper I (Malone *et al.* [19]); i.e., they exclude the uncertainties associated with normalization to absolute DCSs. Thus, the REPs have smaller uncertainties relative to our absolute DCSs.

A. Excitation of the $C^3\Pi_u(v')$ state

Table I displays the DCSs and associated uncertainties for the electron-impact excitation of the $C^3\Pi_u(v')$ state transitions measured in this work ranging from $E_0=13$ to 100 eV. Figure 1 shows the present measurements compared with available data for excitation of the individual $C^3\Pi_u(v')$ state DCSs for $v'=0, 1, 2, 3$, and 4. The full $C^3\Pi_u(v'=0-4)$ state

TABLE I. Differential cross sections for the electron-impact excitation of the $X^1\Sigma_g^+(v''=0) \rightarrow C^3\Pi_u(v')$ transitions in N_2 , where $v' = 0, 1, 2, 3$, and 4. DCSs are given in units of $10^{-20} \text{ cm}^2 \text{ sr}^{-1}$. Also provided are the average percentage uncertainties over all covered angles and at each E_0 .

	Angle (deg)	$C^3\Pi_u(v'=0)$		$C^3\Pi_u(v'=1)$		$C^3\Pi_u(v'=2)$		$C^3\Pi_u(v'=3)$		$C^3\Pi_u(v'=4)$	
		DCS	Error	DCS	Error	DCS	Error	DCS	Error	DCS	Error
(a) $E_0=13 \text{ eV}$	10	62.9	12.0	18.3	3.8	4.60	1.04	1.75	0.44	1.21	0.53
	15	74.6	13.8	24.4	4.9	3.31	0.80	1.27	0.35	0.559	0.242
	20	77.1	14.3	26.9	5.2	4.88	1.03	1.76	0.42	0.684	0.258
	25	80.3	14.8	25.6	5.0	5.36	1.13	2.61	0.60	0.527	0.188
	30	79.1	14.8	26.3	5.0	3.70	0.81	2.43	0.57	0.860	0.370
	35	82.3	15.3	26.1	5.1	3.90	0.84	2.91	0.66	0.939	0.382
	40	76.9	14.4	28.8	5.9	6.49	1.44	2.73	0.66	0.370	0.147
	45	80.2	15.0	20.6	4.2	5.18	1.26	1.99	0.54	1.01	0.33
	50	67.9	12.8	24.5	5.1	7.00	1.64	2.35	0.61	0.812	0.257
	60	66.9	12.6	19.4	4.1	4.61	1.07	2.56	0.65	1.36	0.50
	65	74.6	14.0	20.0	4.2	3.84	0.91	1.93	0.50	1.44	0.43
	70	65.3	12.2	16.2	3.4	3.85	0.92	1.55	0.41	0.509	0.167
	80	59.0	11.2	13.5	2.8	2.95	0.70	1.51	0.39	0.225	0.081
	85	66.6	12.4	18.3	3.8	4.29	1.02	1.47	0.39	0.185	0.072
	90	88.3	16.6	21.6	4.5	3.96	0.92	1.77	0.45	0.308	0.110
	100	88.0	16.6	21.6	4.5	5.65	1.34	1.90	0.50	0.625	0.205
	105	74.4	14.0	18.3	3.8	5.15	1.19	3.21	0.80	0.718	0.274
110	70.8	13.3	18.5	3.9	4.16	0.98	2.61	0.67	0.585	0.188	
120	64.5	12.1	17.9	3.7	3.06	0.74	1.80	0.47	0.606	0.195	
125	60.3	11.4	15.4	3.2	4.66	1.10	3.90	0.98	0.800	0.247	
130	62.3	11.6	18.8	3.9	5.13	1.21	2.35	0.61	0.562	0.182	
	Average error		19%		20%		23%		25%		36%
(b) $E_0=15 \text{ eV}$	10	85.9	13.4	68.7	11.7	31.2	5.7	12.0	2.4	2.81	0.49
	15	93.7	14.6	70.2	11.7	30.4	6.0	9.72	2.11	2.27	0.82
	17	94.5	14.7	72.1	11.7	31.7	5.5	12.2	2.3	4.87	1.48
	20	95.3	14.8	72.3	11.8	34.3	5.9	14.1	2.6	3.58	0.99
	22	86.1	13.6	63.4	10.2	30.8	5.5	11.7	2.2	3.10	1.15
	24	81.3	12.7	65.2	10.7	29.3	5.2	8.95	1.70	3.57	1.25
	26	86.3	13.5	65.4	11.4	29.5	5.5	11.4	2.3	2.79	0.86
	28	85.7	13.4	65.7	11.4	29.7	6.1	11.3	2.6	1.72	0.49
	30	85.7	13.6	63.1	11.1	27.7	5.6	9.92	2.18	3.89	1.02
	32	87.8	13.9	66.1	11.8	29.0	5.7	10.0	2.1	1.96	0.65
	35	88.9	14.0	65.1	11.6	27.4	5.5	9.03	1.97	2.11	0.57
	40	80.7	12.7	57.8	10.1	25.0	5.1	6.39	1.43	2.88	0.77
	45	84.5	13.4	56.0	10.0	25.5	5.1	6.50	1.43	2.02	0.54
	50	79.3	12.4	54.7	9.6	23.6	4.7	5.23	1.17	1.52	0.42
	60	84.5	13.3	54.2	9.6	23.0	4.5	7.50	1.58	1.69	0.44
	65	92.5	14.6	59.0	10.4	23.7	4.7	8.08	1.77	1.36	0.38
	70	99.2	15.7	64.6	11.5	26.2	5.1	6.87	1.48	1.72	0.57
80	112	18	70.2	12.5	26.8	5.3	7.82	1.71	1.68	0.46	
85	116	18	74.2	13.0	29.3	5.9	10.3	2.3	1.41	0.40	
90	114	18	71.9	12.9	28.3	5.7	6.90	1.52	1.87	0.51	
100	91.7	14.3	60.3	10.5	22.3	4.5	6.86	1.52	0.927	0.268	
105	82.1	12.9	54.0	9.5	22.3	4.3	5.80	1.23	1.07	0.29	

TABLE I. (Continued.)

	Angle (deg)	$C^3\Pi_u(v'=0)$		$C^3\Pi_u(v'=1)$		$C^3\Pi_u(v'=2)$		$C^3\Pi_u(v'=3)$		$C^3\Pi_u(v'=4)$	
		DCS	Error	DCS	Error	DCS	Error	DCS	Error	DCS	Error
	110	82.8	13.1	56.2	9.9	22.2	4.3	6.50	1.38	1.20	0.32
	120	88.9	14.0	60.4	10.7	25.4	4.9	8.03	1.70	0.797	0.227
	125	100	16	66.4	11.7	27.1	5.2	8.14	1.72	0.795	0.230
	130	114	18	79.1	14.0	29.8	5.8	9.61	2.03	1.30	0.36
	Average error		16%		17%		19%		21%		29%
(c) $E_0=17.5$ eV	15	52.0	8.0	35.1	5.9	11.1	2.0	3.38	0.63	0.920	0.330
	20	50.9	7.9	30.7	5.1	11.1	2.2	2.37	0.49	1.00	0.34
	25	57.8	8.9	35.5	5.7	12.8	2.2	2.73	0.48	1.02	0.30
	30	57.8	8.9	34.1	5.5	11.2	1.9	2.46	0.44	0.864	0.224
	35	57.9	9.0	35.8	5.7	11.9	2.1	2.19	0.41	0.683	0.245
	40	63.0	9.8	38.9	6.4	12.3	2.1	2.43	0.44	0.758	0.257
	45	68.2	10.6	40.1	6.9	14.5	2.7	3.15	0.62	0.529	0.154
	50	63.6	9.9	36.3	6.3	12.6	2.6	2.63	0.58	0.461	0.119
	60	70.5	11.1	42.4	7.4	14.6	2.9	3.09	0.66	0.464	0.115
	65	76.5	12.0	46.0	8.1	15.8	3.1	4.07	0.85	0.526	0.165
	70	82.1	12.9	51.7	9.2	16.0	3.2	3.24	0.69	0.721	0.177
	80	90.3	14.1	54.6	9.5	19.1	3.8	4.50	0.97	0.994	0.250
	85	82.0	13.0	54.0	9.6	19.1	3.8	3.88	0.83	0.828	0.204
	90	76.4	11.9	47.9	8.3	16.3	3.2	2.86	0.61	1.11	0.28
	100	64.2	10.1	41.8	7.3	15.8	3.0	3.41	0.70	0.819	0.193
	105	61.0	9.6	37.1	6.5	13.7	2.7	3.15	0.67	0.787	0.195
	110	58.9	9.3	37.2	6.6	12.1	2.3	3.25	0.68	0.847	0.265
	120	56.9	8.9	38.0	6.7	14.0	2.8	4.14	0.88	0.874	0.215
	125	61.5	9.6	39.1	6.8	16.2	3.2	3.45	0.75	1.10	0.28
	130	71.4	11.3	45.0	8.0	16.5	3.3	4.08	0.87	1.08	0.27
	Average error		16%		17%		19%		20%		28%
(d) $E_0=20$ eV	5	24.1	3.7	17.9	3.0	9.50	1.67	2.90	0.54	0.643	0.224
	10	31.1	4.8	23.4	3.9	10.0	1.9	3.23	0.66	0.557	0.183
	15	38.2	5.9	27.8	4.5	10.9	1.8	2.90	0.51	0.469	0.133
	17	43.3	6.6	28.1	4.5	11.9	2.0	3.02	0.53	0.541	0.136
	20	48.5	7.6	33.8	5.3	12.4	2.2	3.80	0.70	0.768	0.267
	22	47.5	7.3	32.4	5.3	13.4	2.3	3.93	0.70	0.705	0.232
	24	48.5	7.5	31.5	5.4	14.4	2.6	4.18	0.80	0.949	0.269
	26	45.8	7.1	33.1	5.7	14.5	2.9	4.38	0.95	0.726	0.183
	28	51.0	8.0	32.0	5.5	14.1	2.7	4.48	0.94	0.642	0.156
	30	50.9	8.0	34.8	6.1	15.6	3.0	3.86	0.79	0.616	0.187
	32	50.9	8.0	33.2	5.8	13.5	2.6	4.11	0.86	0.839	0.201
	35	47.8	7.5	32.8	5.7	13.2	2.6	3.62	0.77	0.826	0.203
	40	49.5	7.8	30.3	5.3	13.3	2.6	4.14	0.86	0.669	0.161
	45	48.7	7.5	32.4	5.6	12.5	2.4	3.55	0.75	0.820	0.200
	50	48.4	7.6	31.1	5.4	12.4	2.3	3.57	0.72	0.807	0.186
	60	53.3	8.4	34.9	6.1	13.4	2.6	3.87	0.81	0.654	0.158
	65	57.2	9.0	35.6	6.2	13.5	2.6	3.59	0.73	0.575	0.175
	70	60.2	9.4	37.5	6.6	14.1	2.7	3.90	0.81	0.556	0.134
	80	67.8	10.6	43.5	7.5	16.4	3.2	3.80	0.80	0.814	0.200

TABLE I. (*Continued.*)

Angle (deg)	$C^3\Pi_u(v'=0)$		$C^3\Pi_u(v'=1)$		$C^3\Pi_u(v'=2)$		$C^3\Pi_u(v'=3)$		$C^3\Pi_u(v'=4)$		
	DCS	Error	DCS	Error	DCS	Error	DCS	Error	DCS	Error	
85	64.5	10.2	41.2	7.2	15.4	3.0	4.55	0.95	0.796	0.192	
90	58.5	9.1	37.5	6.4	14.1	2.8	3.89	0.82	0.971	0.236	
100	54.3	8.5	33.3	5.8	12.2	2.3	3.16	0.64	0.939	0.216	
105	54.9	8.6	34.2	5.9	14.5	2.7	3.55	0.72	1.11	0.25	
110	54.6	8.5	33.8	5.9	13.6	2.6	3.46	0.70	1.12	0.26	
120	57.1	8.9	35.2	6.1	14.2	2.7	3.87	0.78	0.952	0.219	
125	59.0	9.2	35.9	6.2	15.0	2.8	4.21	0.85	0.947	0.218	
130	57.5	9.0	36.0	6.3	14.5	2.7	4.09	0.82	0.701	0.161	
Average error		16%		17%		19%		20%		26%	
(e) $E_0=25$ eV	10	12.5	1.9	6.64	1.11	1.76	0.31	2.44	0.63	0.575	0.216
	15	10.7	1.6	5.55	0.92	3.25	0.63	2.54	0.53	1.14	0.39
	20	8.74	1.35	5.18	0.83	2.39	0.41	1.67	0.29	0.875	0.255
	25	12.1	1.9	6.57	1.06	2.62	0.45	1.44	0.26	0.566	0.147
	30	16.9	2.6	8.35	1.33	2.83	0.50	2.14	0.40	0.765	0.275
	35	17.1	2.7	12.2	2.0	2.79	0.48	1.62	0.29	0.821	0.278
	40	21.1	3.3	11.4	2.0	3.80	0.70	2.32	0.45	1.19	0.35
	45	22.6	3.5	10.0	1.7	6.13	1.25	2.24	0.49	1.05	0.27
	50	22.6	3.6	12.6	2.2	7.81	1.55	2.08	0.44	1.24	0.31
	60	23.8	3.7	15.2	2.7	7.30	1.42	2.07	0.43	0.906	0.284
	65	30.4	4.8	20.2	3.6	9.16	1.80	2.62	0.56	1.15	0.28
	70	28.4	4.5	16.5	2.9	11.2	2.2	2.34	0.50	0.824	0.207
	80	30.2	4.8	23.0	4.1	9.61	1.90	1.60	0.34	1.19	0.29
	85	27.4	4.3	20.6	3.6	8.99	1.79	2.63	0.56	1.32	0.33
	90	26.1	4.1	21.2	3.7	8.88	1.70	2.70	0.55	1.02	0.24
	100	34.8	5.5	19.9	3.5	7.98	1.58	3.16	0.68	1.82	0.45
	105	33.1	5.2	25.6	4.5	12.4	2.4	3.26	0.68	1.48	0.46
	110	34.1	5.3	20.4	3.6	12.5	2.5	4.24	0.90	1.45	0.36
	120	38.2	6.0	30.2	5.3	12.1	2.4	3.06	0.66	1.11	0.28
	125	44.9	7.1	30.2	5.4	12.9	2.6	2.90	0.62	1.38	0.34
	130	44.5	6.9	29.6	5.1	13.8	2.7	3.41	0.73	1.32	0.33
Average error		16%		17%		19%		21%		28%	
(f) $E_0=30$ eV	5	20.3	3.1	9.01	1.50	2.45	0.48	0.119	0.022	0.202	0.042
	10	20.8	3.2	7.24	1.19	2.01	0.38	0.176	0.036	0.174	0.041
	15	17.0	2.6	8.07	1.30	2.42	0.41	0.327	0.057	0.226	0.072
	20	18.2	2.8	7.50	1.20	1.91	0.32	0.299	0.053	0.244	0.062
	25	21.7	3.4	10.5	1.7	2.61	0.46	0.362	0.066	0.336	0.068
	30	22.4	3.5	12.0	1.9	2.82	0.48	0.668	0.119	0.277	0.054
	35	16.6	2.6	8.78	1.50	2.51	0.46	0.706	0.136	0.236	0.067
	40	21.2	3.3	10.9	1.9	3.29	0.66	1.03	0.22	0.381	0.096
	45	23.2	3.6	12.1	2.1	4.04	0.79	0.671	0.141	0.346	0.084
	50	20.7	3.2	10.9	1.9	4.03	0.77	1.00	0.21	0.336	0.102
	60	29.4	4.6	17.7	3.1	5.43	1.05	1.16	0.24	0.352	0.084
	65	26.9	4.2	15.6	2.7	6.12	1.21	1.54	0.33	0.496	0.122
	70	28.9	4.6	17.7	3.1	6.15	1.20	1.71	0.36	0.497	0.120
	80	29.5	4.6	18.3	3.1	6.79	1.33	1.26	0.27	0.332	0.081

TABLE I. (Continued.)

Angle (deg)	$C^3\Pi_u(v'=0)$		$C^3\Pi_u(v'=1)$		$C^3\Pi_u(v'=2)$		$C^3\Pi_u(v'=3)$		$C^3\Pi_u(v'=4)$		
	DCS	Error	DCS	Error	DCS	Error	DCS	Error	DCS	Error	
85	27.7	4.3	17.5	3.1	7.00	1.32	1.54	0.31	0.294	0.068	
90	29.2	4.6	15.8	2.7	6.45	1.26	1.40	0.29	0.258	0.062	
100	30.7	4.8	18.2	3.2	6.19	1.18	1.20	0.25	0.383	0.116	
105	31.5	4.9	19.3	3.4	6.38	1.24	1.80	0.37	0.243	0.058	
110	32.6	5.1	18.3	3.2	6.13	1.21	1.67	0.35	0.269	0.066	
120	36.9	5.8	20.4	3.6	5.32	1.03	1.67	0.35	0.160	0.039	
125	36.6	5.7	21.7	3.7	5.25	1.03	1.89	0.40	0.160	0.039	
130	39.5	6.2	22.5	3.9	5.14	0.97	1.64	0.33	0.163	0.038	
Average error		16%		17%		19%		20%		25%	
(g) $E_0=50$ eV	5	6.87	1.06	5.08	0.86	1.17	0.21	0.777	0.154	0.124	0.028
	10	14.6	2.3	7.63	1.27	2.35	0.46	1.45	0.33	0.268	0.070
	15	11.4	1.8	5.65	0.92	3.01	0.51	0.973	0.179	0.284	0.104
	20	9.63	1.48	5.37	0.87	1.78	0.31	0.598	0.111	0.0897	0.0255
	25	13.7	2.1	6.70	1.07	1.90	0.34	0.453	0.088	0.129	0.029
	30	11.2	1.7	6.44	1.06	1.75	0.30	0.607	0.115	0.127	0.027
	35	9.73	1.52	5.43	0.95	0.980	0.182	0.425	0.088	0.117	0.038
	40	9.98	1.56	5.63	0.98	1.23	0.25	0.263	0.063	0.286	0.081
	45	7.58	1.20	5.08	0.90	1.32	0.27	0.370	0.085	0.150	0.041
	50	10.4	1.6	5.72	1.02	1.01	0.20	0.557	0.124	0.246	0.086
	60	9.10	1.43	5.58	1.00	1.77	0.35	0.348	0.079	0.173	0.047
	65	10.6	1.7	5.04	0.89	1.57	0.32	0.466	0.108	0.107	0.029
	70	7.89	1.25	4.36	0.78	1.12	0.22	0.469	0.107	0.208	0.056
	80	11.4	1.8	6.48	1.13	1.89	0.38	0.618	0.143	0.400	0.109
	85	12.6	2.0	5.59	0.99	1.61	0.31	0.525	0.115	0.0981	0.0251
	90	12.8	2.0	6.13	1.08	2.28	0.46	0.474	0.109	0.103	0.028
	100	12.5	2.0	8.94	1.60	1.82	0.36	0.566	0.126	0.124	0.043
	105	14.0	2.2	8.13	1.46	1.78	0.36	0.387	0.088	0.0626	0.0168
	110	12.3	1.9	6.97	1.23	2.14	0.43	0.358	0.083	0.0572	0.0158
	120	13.1	2.1	7.20	1.29	1.26	0.25	0.643	0.147	0.215	0.058
	125	14.6	2.3	7.72	1.35	1.31	0.26	0.505	0.117	0.294	0.080
	130	13.7	2.1	7.88	1.40	2.25	0.31	0.491	0.108	0.249	0.064
Average error			16%		17%		19%		22%		28%
(h) $E_0=100$ eV	5	1.56	0.24	0.646	0.109	0.283	0.051	0.0896	0.0177	0.0133	0.0030
	10	2.69	0.42	1.44	0.24	0.635	0.125	0.123	0.028	0.0203	0.0053
	15	4.86	0.75	2.75	0.45	0.902	0.154	0.156	0.029	0.0210	0.0077
	20	6.94	1.07	3.60	0.58	1.20	0.21	0.185	0.034	0.0346	0.0098
	30	6.57	1.03	3.67	0.59	1.33	0.24	0.206	0.040	0.0504	0.0111
	40	4.63	0.72	2.53	0.42	0.884	0.154	0.172	0.033	0.0403	0.0086
	50	2.91	0.46	1.53	0.27	0.582	0.108	0.111	0.023	0.0215	0.0069
	60	2.31	0.36	1.19	0.21	0.468	0.097	0.0905	0.0216	0.0107	0.0031
	70	1.63	0.26	0.912	0.161	0.339	0.068	0.0837	0.0192	0.00806	0.00219
	80	1.21	0.19	0.754	0.135	0.243	0.048	0.0855	0.0191	0.00838	0.00292
	90	1.00	0.16	0.640	0.115	0.205	0.041	0.0647	0.0147	0.00952	0.00256

TABLE I. (*Continued.*)

Angle (deg)	$C^3\Pi_u(v'=0)$		$C^3\Pi_u(v'=1)$		$C^3\Pi_u(v'=2)$		$C^3\Pi_u(v'=3)$		$C^3\Pi_u(v'=4)$	
	DCS	Error	DCS	Error	DCS	Error	DCS	Error	DCS	Error
100	0.900	0.141	0.534	0.094	0.195	0.040	0.0728	0.0170	0.00979	0.00270
110	0.930	0.148	0.412	0.074	0.173	0.035	0.0808	0.0185	0.00950	0.00257
120	0.979	0.153	0.491	0.086	0.152	0.031	0.0650	0.0150	0.00961	0.00263
130	1.67	0.26	0.868	0.154	0.254	0.049	0.0695	0.0152	0.00875	0.00224
Average error		16%		17%		19%		21%		28%

DCSs are discussed in more detail in Paper I (Ref. [19]) but are also included in Fig. 1.

At $E_0=13$ eV, the present DCSs are compared with experimentally obtained single DCS values at $\theta=90^\circ$. As shown in Fig. 1, the $E_0=13$ eV panel includes the DCS results of Zobel *et al.* (see LeClair and Trajmar [20]) for $v'=0-2$ at 13 eV (the topmost datum of Zobel *et al.* in Fig. 1), which reveals a slight disagreement with the present DCS at 90° . This slight difference is primarily due to the significance of the $v'=3$ DCS relative to the $v'=2$ DCS at this E_0 . Also shown are the $v'=0$ DCS of Zobel *et al.* (see Ref. [20]) at $E_0=11.6, 12, 12.5,$ and 13 eV, respectively, increasing in magnitude with E_0 from the lowest DCS datum on Fig. 1. The results of Zobel *et al.* (see Ref. [20]) indicate a steep rise from threshold via the increasing $C^3\Pi_u$ state DCSs (for $v'=0-2$) and are in excellent agreement with the present DCS at 90° . Also shown are the 90° DCSs of LeClair and Trajmar [20] at a smaller E_0 (12 eV) for $v'=0-2$ (higher datum) and $v'=0$ (lower datum). Furthermore, we note that core excited resonances have been listed by Mazeau *et al.* [21] at 12.54 eV ($^2\Pi_u$) and 13.00 eV ($^2\Sigma_u^-$) for the $C^3\Pi_u(v'=0)$ state, which could result in near-threshold intensity variations between the data sets due to energy calibration uncertainties (e.g., E_0 and resolution).

Figure 1 also shows the present DCSs at $E_0=15$ eV compared with the 90° DCS data from Zobel *et al.* (actually at 14.8 eV, see Ref. [20]) for $v'=0-2$ (higher datum) and $v'=0$ (lower datum) along with the DCSs of LeClair and Trajmar [20] at 15 eV for $v'=0-3$ (higher datum) and $v'=0$ (lower datum). As expected, the uniform transmission results of LeClair and Trajmar [20], for the essentially full $C^3\Pi_u(v'=0-3)$ state, is consistent with the present result at 90° , as is the DCS of the $v'=0$ level. The data of Zobel *et al.* (see Ref. [20]) are slightly larger but agree well within experimental uncertainties.

At $E_0=17.5$ eV, the present DCSs are compared with experimental data from Zubek and King [18], who correctly did not apply FCFs in unfolding their energy-loss data at $E_0=17.5$ and 20 eV. The Zubek and King [18] DCSs were measured for the essentially full $C^3\Pi_u(v'=0-3)$ state (higher data set) and $v'=0$ level (lower data set), which both agree excellently with the present $C^3\Pi_u$ state DCSs. However, some deviation is apparent for $\theta>90^\circ$. Additional discussion of Zubek and King [18], along with Zobel *et al.* (see Ref. [20]) and LeClair and Trajmar [20], can be found in Paper I (Ref. [19]). Similarly, the present DCSs at

$E_0=20$ eV are compared with data from Zubek and King [18] with the same excellent agreement evident at $E_0=17.5$ eV. The $E_0=20$ eV panel of Fig. 1 includes the 90° DCS value of LeClair and Trajmar [20] at 20.7 eV for the nearly full $C^3\Pi_u(v'=0-2)$ state (higher datum) and $v'=0$ (lower datum) level. The agreement is very good with both DCSs being slightly lower, but within uncertainties, where the slight difference is due to partial vibrational coverage ($v'=0-2$) of the full state and slight variance in the different elastic DCSs used in normalizing the respective data sets. This appears to correspond to the fall-off in intensity associated with the excitation (integral) cross section, which occurs as E_0 increases beyond the cross-section maximum.

Besides the full $C^3\Pi_u(v'=0-4)$ state DCSs, as discussed in Paper I (Ref. [19]), we are not aware of other direct excitation data for direct comparison with our present results for $E_0>20$ eV. Figure 1 illustrates general trends in our data. The shapes of the DCSs frequently show correlated structure as a function of scattering angle. The $E_0=100$ eV data nicely illustrate this commonly evolving shape. However, the $v'=3$ and 4 (and sometimes $v'=2$) levels are prone to large intensity deviations in their DCS values even within local angular ranges, which is largely due to a greater degree of uncertainty in the unfolding process. Also, shape deviations with respect to the more intense features are sometimes observed. The $C^3\Pi_u$ state is electrostatically coupled to the $C^3\Pi_u$ valence-state continuum (see the recent coupled-channels study by Lewis *et al.* [17]), which could be responsible for our observations. The $v'=3$ and 4 level DCSs are very weak in magnitude, as was the case at smaller E_0 , relative to the DCSs of the $v'=0$ and 1 levels with the intensity of the $C^3\Pi_u(v'=2)$ level generally falling between the two sets. The relative intensities for excitation of the $C^3\Pi_u(v')$ levels are the subject of Sec. III B.

B. Relative excitation probabilities

Figure 1 consistently shows the present $C^3\Pi_u(v')$ level DCSs differing by 2–3 orders of magnitude for all investigated E_0 (13–100 eV), particularly near threshold. Thus the majority of the full $C^3\Pi_u(v'=0-4)$ intensity is due to the $v'=0$ and 1 levels. Table II provides the REPs, stated as percentages, for the $X^1\Sigma_g^+(v''=0)\rightarrow C^3\Pi_u(v')$ transitions relative to the $C^3\Pi_u(v'=0-4)$ sum.

The REPs were obtained by averaging the present relative vibronic intensities. In order to preclude overweighting of

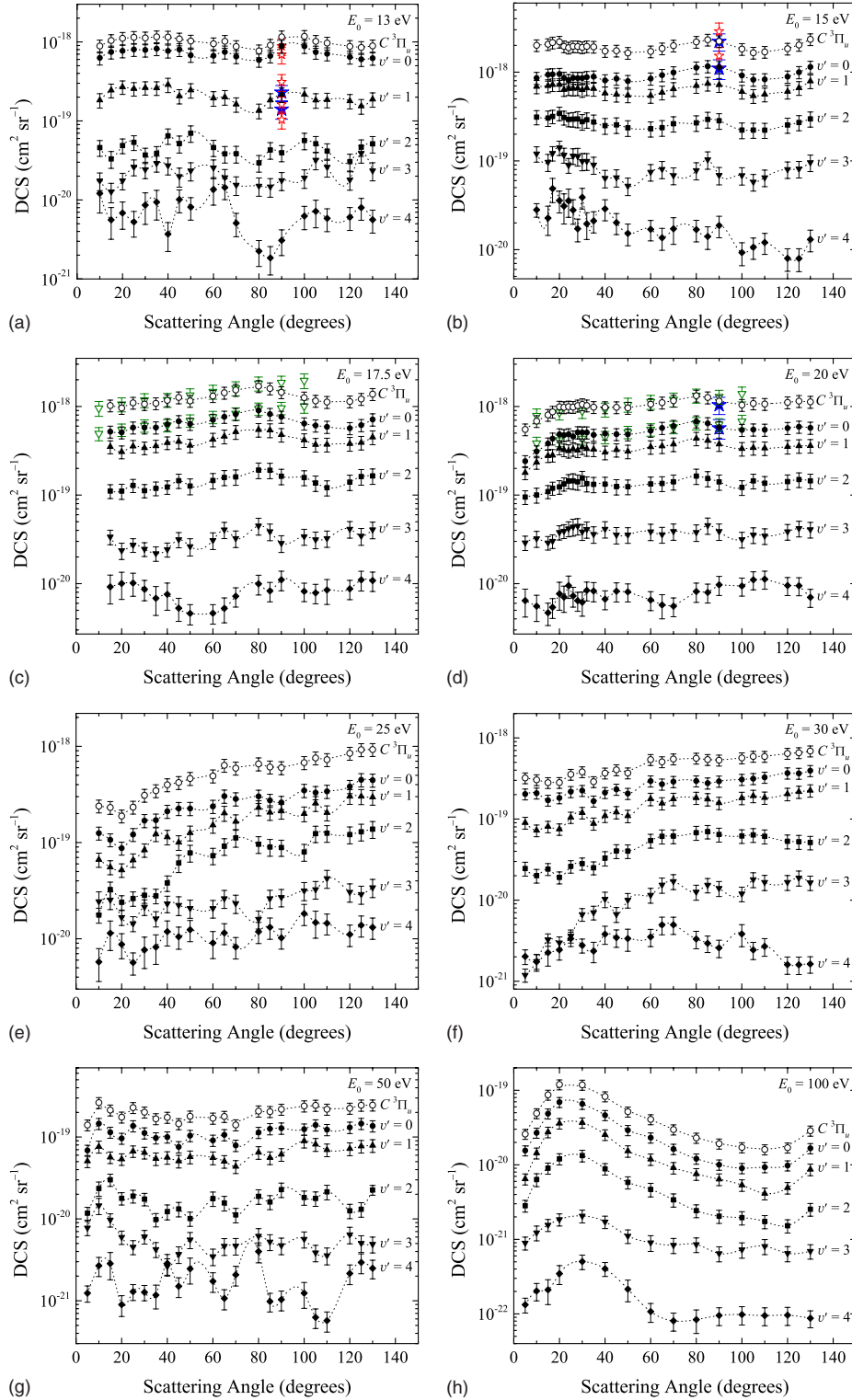


FIG. 1. (Color online) DCSs for the electron-impact excitations to the $C^3\Pi_u(v')$ state with E_0 and v' indicated in the figure panels. The single DCS values at $\theta=90^\circ$ on several panels are identified as follows. The $E_0=13$ eV panel includes the Zobel *et al.* (see LeClair and Trajmar [20]) DCSs for $v'=0-2$ (top) and the $v'=0$ data, which are 11.6, 12, 12.5, and 13 eV, respectively, from bottom upward. Also shown are the 90° DCSs of LeClair and Trajmar [20] at 12 eV for $v'=0-2$ (high) and $v'=0$ (low). The $E_0=15$ eV panel includes the data of Zobel *et al.* at 14.8 eV for $v'=0-2$ (high) and $v'=0$ (low) along with the DCSs of LeClair and Trajmar [20] at 15 eV for $v'=0-3$ (high) and $v'=0$ (low). The $E_0=20$ eV panel includes the 90° DCS value of LeClair and Trajmar [20] at 20.7 eV for $v'=0-2$ (high) and $v'=0$ (low). Legend: \circ , present work ($v'=0-4$); \bullet , present work ($v'=0$); \blacktriangle , present work ($v'=1$); \blacksquare , present work ($v'=2$); \blacktriangledown , present work ($v'=3$); \blacklozenge , present work ($v'=4$); ∇ , Zubek and King [18] (data sets: $v'=0-3$ high and $v'=0$ low); \star , LeClair and Trajmar [20]; and \star , Zobel *et al.* (see LeClair and Trajmar [20]). The dotted lines for the present data are intended to guide the eye. DCS units are in $\text{cm}^2 \text{sr}^{-1}$. See text for further details.

TABLE II. Present REPs, stated in the form of percentages, for vibrational levels of the $C^3\Pi_u$ state relative to the full $C^3\Pi_u(v'=0-4)$ state excitation. The REPs were obtained by averaging the mean relative vibronic intensities within 10° intervals. See text for further details.

v'	Present $C^3\Pi_u$ average relative excitation probabilities (%)															
	13 eV	Error	15 eV	Error	17.5 eV	Error	20 eV	Error	25 eV	Error	30 eV	Error	50 eV	Error	100 eV	Error
0	71.90	4.09	48.27	2.87	52.66	2.03	49.93	1.85	48.22	1.88	57.03	2.33	56.18	2.56	56.02	3.41
1	20.60	2.25	32.97	3.11	32.76	2.42	32.37	2.26	30.24	2.17	30.52	2.28	31.59	2.60	29.93	3.03
2	4.61	0.75	13.67	1.64	11.33	1.20	13.22	1.26	14.12	1.49	9.60	1.05	8.47	1.03	10.72	1.64
3	2.21	0.43	4.14	0.59	2.58	0.35	3.70	0.45	5.18	0.63	2.20	0.32	2.85	0.50	2.91	0.71
4	0.68	0.22	0.95	0.21	0.67	0.15	0.78	0.16	2.24	0.44	0.65	0.16	0.91	0.25	0.42	0.22
Sum	100.00	4.75	100.00	4.58	100.00	3.40	100.00	3.22	100.00	3.33	100.00	3.44	100.00	3.83	100.00	4.90

the averaged intensities by the irregular density of angular measurements (see Fig. 1) taken in our experiment, the angular range was divided into 10° intervals. The REPs were then calculated by averaging the mean value of the intensities measured within each interval. Of note here is that the determined REPs would be equivalent to FCFs if the Franck-Condon principle remained valid.

The REPs at $E_0=100$ and 50 eV, listed in Table II, agree excellently, within our experimental uncertainties, with the FCFs tabulated in Lofthus and Krupenie [13] and Gilmore *et al.* [22]. Though this agreement is excellent, we caution against the use of intensity ratios of the present results at a particular scattering angle as “effective FCFs,” especially for the weaker intensities (i.e., $v'=4, 3,$ and 2). While the global

averaging method generates ratios consistent with published FCFs, the relative DCSs for vibrational levels in the electronic manifold of the $C^3\Pi_u$ state show some scatter over the observed scattering angular range as expected when the Franck-Condon principle is inapplicable.

The present REPs listed in Table III have been renormalized to facilitate comparison with other data sets. Here, we have divided the FCFs by their respective $C^3\Pi_u(v'=0)$ intensity in order to compare other data sets that did not include higher vibrational levels. Table III shows the present ratios, relative to the $v'=0$ level, for each of our experimental E_0 . Table III provides the relative comparisons of the present data to available FCFs for the excitation of the $X^1\Sigma_g^+(v''=0) \rightarrow C^3\Pi_u(v')$ transitions in N_2 . Again, the data

TABLE III. (a) Comparisons of the present REPs, adapted from Table II, for vibrational levels of the $C^3\Pi_u$ state normalized to the $C^3\Pi_u(v'=0)$ level and (b) relative comparisons of the present data to available REPs and Franck-Condon factors (indicated as optical) for the excitation of the $X^1\Sigma_g^+(v''=0) \rightarrow C^3\Pi_u(v')$ transitions in N_2 .

(a) Normalized present $C^3\Pi_u$ relative excitation probabilities																
v'	13 eV	Error	15 eV	Error	17.5 eV	Error	20 eV	Error	25 eV	Error	30 eV	Error	50 eV	Error	100 eV	Error
0	1.000	0.057	1.000	0.059	1.000	0.039	1.000	0.037	1.000	0.039	1.000	0.041	1.000	0.046	1.000	0.061
1	0.286	0.031	0.683	0.064	0.622	0.046	0.648	0.045	0.627	0.045	0.535	0.040	0.562	0.046	0.534	0.054
2	0.064	0.010	0.283	0.034	0.215	0.023	0.265	0.025	0.293	0.031	0.168	0.018	0.151	0.018	0.191	0.029
3	0.031	0.006	0.086	0.012	0.049	0.007	0.074	0.009	0.107	0.013	0.038	0.006	0.051	0.009	0.052	0.013
4	0.009	0.003	0.020	0.004	0.013	0.003	0.016	0.003	0.046	0.009	0.011	0.003	0.016	0.005	0.008	0.004

(b) Normalized $C^3\Pi_u$ relative excitation probabilities								
v'	PVB ^a 14–14.5 eV		ZK ^b 17.5 eV		ZK ^b 20 eV		LK ^c <i>Optical</i>	GLE ^d <i>Optical</i>
0	1.000		1.000		1.000		1.000	1.000
1	0.681		0.620		0.666		0.558	0.565
2	0.349		0.230		0.280		0.193	0.194
3			0.066		0.085		0.054	0.055
4							0.014	0.014

^aReference [23].

^bReference [18].

^cReference [13].

^dReference [22].

of Lofthus and Krupenie [13] and Gilmore *et al.* [22], which are “optical” (i.e., equivalent to large E_0), demonstrate excellent agreement (within our uncertainties) with the present results at $E_0=100$ and 50 eV.

Below approximately 50 eV, there is clear disagreement between the present values and the optical FCF results, showing some departure from the Franck-Condon principle. We note that the DCSs have consistently evolving shapes as a function of scattering angle as shown in Fig. 1. The accuracy of the present results are substantiated by a comparison with the data of Poparic *et al.* [23] and Zubek and King [18] in Table III. The fixed-angle excitation functions of Poparic *et al.* [23] indicated maxima in the measured intensities of the $v'=0, 1$, and 2 levels in the range $E_0=14-14.5$ eV. These peak values were used to construct their tabulated REP ratios. The agreement is excellent for the $v'=0$ and 1 results, while the intensity ratio for $v'=2$ is in poor agreement. (Interestingly, the sum of our ratios for $v'=2-4$ agrees with the $v'=2$ result of Poparic *et al.* [23].) Zubek and King [18] acquired DCSs at $E_0=17.5$ and 20 eV, such that their REP ratios were obtained from Table 2 in their article. Minimal disagreement outside of *our* uncertainty is seen for $v'=3$, but the $v'=0-2$ results are in excellent agreement.

IV. CONCLUSIONS

Vibrationally resolved DCSs for electron impact excitation of the $C^3\Pi_u(v')$ state from the $X^1\Sigma_g^+(v''=0)$ ground-state level in N_2 were obtained from the energy-loss spectra. The individual DCSs for the $v'=0, 1, 2, 3$, and 4 levels are presented here and compared with available data sets demonstrating excellent agreement in most cases. Furthermore, we have obtained REPs for the $X^1\Sigma_g^+(v''=0) \rightarrow C^3\Pi_u(v')$ transitions in N_2 . Our average relative vibronic intensities (i.e., REPs) of the $C^3\Pi_u$ state demonstrate some departure from the Franck-Condon principle for excitation energies less than 50 eV. The DCSs of the full $C^3\Pi_u(v'=0-4)$ state are discussed in detail in Part I (Malone *et al.* [19]).

ACKNOWLEDGMENTS

This work was performed at the California State University, Fullerton and at the Jet Propulsion Laboratory, California Institute of Technology under a contract with the National Aeronautics and Space Administration (NASA). We gratefully acknowledge financial support through the National Science Foundation under Grant No. NSF-PHY-RUI-0653452, and NASA’s Outer Planets and Planetary Atmospheres Research programs.

-
- [1] Y. Itikawa, J. Phys. Chem. Ref. Data **35**, 31 (2006).
 [2] Y. Itikawa, M. Hayashi, A. Ichimura, K. Onda, K. Sakimoto, K. Takayanagi, M. Nakamura, H. Nishimura, and T. Takayanagi, J. Phys. Chem. Ref. Data **15**, 985 (1986).
 [3] M. Sataka and H. Kubo, Fusion Sci. Technol. **51**, 135 (2007).
 [4] T. Tabata, T. Shirai, M. Sataka, and H. Kubo, At. Data Nucl. Data Tables **92**, 375 (2006).
 [5] M. Tashiro and K. Morokuma, Phys. Rev. A **75**, 012720 (2007).
 [6] R. F. da Costa and M. A. P. Lima, Int. J. Quantum Chem. **106**, 2664 (2006).
 [7] R. F. da Costa and M. A. P. Lima, Phys. Rev. A **75**, 022705 (2007).
 [8] P. V. Johnson, C. P. Malone, I. Kanik, K. Tran, and M. A. Khakoo, J. Geophys. Res. **110**, A11311 (2005).
 [9] M. A. Khakoo, P. V. Johnson, I. Ozkay, P. Yan, S. Trajmar, and I. Kanik, Phys. Rev. A **71**, 062703 (2005).
 [10] M. A. Khakoo, C. P. Malone, P. V. Johnson, B. R. Lewis, R. Laher, S. Wang, V. Swaminathan, D. Nuyujukian, and I. Kanik, Phys. Rev. A **77**, 012704 (2008).
 [11] M. A. Khakoo, S. Wang, R. Laher, P. V. Johnson, C. P. Malone, and I. Kanik, J. Phys. B **40**, F167 (2007).
 [12] C. P. Malone, P. V. Johnson, I. Kanik, B. Ajdari, and M. A. Khakoo, J. Chem. Phys. (to be published).
 [13] A. Lofthus and P. H. Krupenie, J. Phys. Chem. Ref. Data **6**, 113 (1977).
 [14] M. J. Brunger and P. J. O. Teubner, Phys. Rev. A **41**, 1413 (1990).
 [15] D. C. Cartwright, A. Chutjian, S. Trajmar, and W. Williams, Phys. Rev. A **16**, 1013 (1977).
 [16] S. Trajmar, D. F. Register, and A. Chutjian, Phys. Rep. **97**, 219 (1983).
 [17] B. R. Lewis, S. T. Gibson, W. Zhang, H. Lefebvre-Brion, and J. M. Robbe, J. Chem. Phys. **122**, 144302 (2005).
 [18] M. Zubek and G. C. King, J. Phys. B **27**, 2613 (1994).
 [19] C. P. Malone, P. V. Johnson, I. Kanik, B. Ajdari, and M. A. Khakoo, preceding paper, Phys. Rev. A **79**, 032704 (2009).
 [20] L. R. LeClair and S. Trajmar, J. Phys. B **29**, 5543 (1996).
 [21] J. Mazeau, R. I. Hall, G. Joyez, M. Landau, and J. Reinhard, J. Phys. B **6**, 873 (1973).
 [22] F. R. Gilmore, R. R. Laher, and P. J. Espy, J. Phys. Chem. Ref. Data **21**, 1005 (1992).
 [23] G. Poparic, M. Vivic, and D. S. Belic, Chem. Phys. **240**, 283 (1999).